Neoclassical and turbulent transport of W in toroidally rotating JET plasmas

C. Angioni[1], P. Mantica[2], M. Valisa[3], M. Baruzzo [3], E. Belli[4], P. Belo[5], M. Beurskens[6], F. J. Casson[1], C. Challis [6], C. Giroud[6], N. Hawkes[6], T.C. Hender [6], J. Hobirk[1], E. Joffrin[7], L. Lauro Taroni[3], M. Lehnen[8], J. Mlynar[9], T. Pütterich[1], and JET EFDA contributors [1*]

JET-EFDA, Culham Science Centre, Abingdon, OX14 3DB, UK
[1] *Max-Planck Institut für Plasmaphysik, IPP–Euratom Ass., Garching, Germany*
[2] *Istituto di Fisica del Plasma, Associazione Euratom–ENEA–CNR, Milano, Italy*
[3] *Consorzio RFX, Associazione Euratom–ENEA sulla Fusione, I-35127 Padova, Italy*
[4] *General Atomics, PO Box 85608, San Diego, CA 92186-5608, USA*
[5] *EURATOM/IST Fusion Ass., Inst. de Plasma e Fušao Nucl., Lisbon, Portugal*
[6] *EURATOM/CCFE Fusion Ass., Culham Science Centre, Abingdon, OX14 3DB, UK*
[7] *IRFM-CEA, Association Euratom-CEA, Centre de Cadarache, France*
[8] *Forschungszentrum Jülich GmbH, Association EURATOM-FZJ, Jülich, Germany*
[9] *EURATOM-IPP.CR Ass., Inst. of Plasma Physics AS CR, Prague, Czech Republic.*

The physical understanding of the transport of heavy impurities, like W, is important for the achievement of practical fusion energy (see also [1]). Among the plasma parameters which affect impurity transport, rotation has only recently received the deserved consideration [2-6]. In addition to the off-diagonal contribution related to the presence of a radial gradient of the toroidal rotation (usually dubbed roto–diffusion) [2,4,6], even in moderately rotating plasmas, centrifugal effects of heavy impurities become non-negligible [2,3,5]. Plasmas obtained in the hybrid scenario in JET with the ITER-like wall (JET-ILW) can be used to study these effects on W, since the deuterium toroidal rotation reaches central thermal Mach numbers around 0.4 (Mach of W up to 3.8). At the same time, this study allows us to explore the transport mechanisms which are responsible for the central W accumulation which is often observed in this type of discharges [7].

1. Calculations of neoclassical and turbulent transport of W

Calculations of W neoclassical and turbulent transport of two time slices of a JET-ILW hybrid scenario discharge ♯82722 have been performed with the drift-kinetic (DK) code NEO [8] and the gyrokinetic (GK) code GKW [3,9] respectively. The codes NEO and GKW include the consistent treatment of the poloidal asymmetry of the W density due to centrifugal effects. GK calculations are linear. The two time slices have been selected to be representative of two conditions during the time evolution of the high power phase of the discharge. The first at 5.9 s before the start of W accumulation, and the second at 7.5 s during the W accumulation phase. In the calculations, a single W species is considered, with charge which changes along the minor radius and it is given by the local average over the concentrations of all the W ionization stages. Neoclassical and turbulent transport are summed in order to obtain a prediction of the profile at the low field side (LFS) of the normalized logarithmic gradient of W density $R/L_{nW} = -RV_{W\,TOT}/D_{W\,TOT}$, where $RV_{W\,TOT} = RV_{W\,NEO} + RV_{W\,GKW}$ and $D_{W\,TOT} = D_{W\,NEO} + D_{W\,GKW}$ and indexes 'NEO' and 'GKW' indicate the neoclassical and the turbulent components respectively. Given the sensitivity of the GK results to the input gradients, the sum of the neoclassical and turbulent components is performed by imposing that the turbulent ion heat conductivity predicted by the GK calculations $\chi_{i\,\mathrm{GKW}}$ matches the anomalous part of the ion heat conductivity $\chi_{i\,an} = \chi_{i\,PB} - \chi_{i\,NEO}$. Here $\chi_{i\,PB}$ is the power balance ion heat conductivity obtained by interpretive JETTO calculations [7]. Then, the expression for the LFS value

[1*] See the Appendix of F. Romanelli et al., Proceedings of the 24th IAEA Fusion Energy Conference 2012, San Diego, US

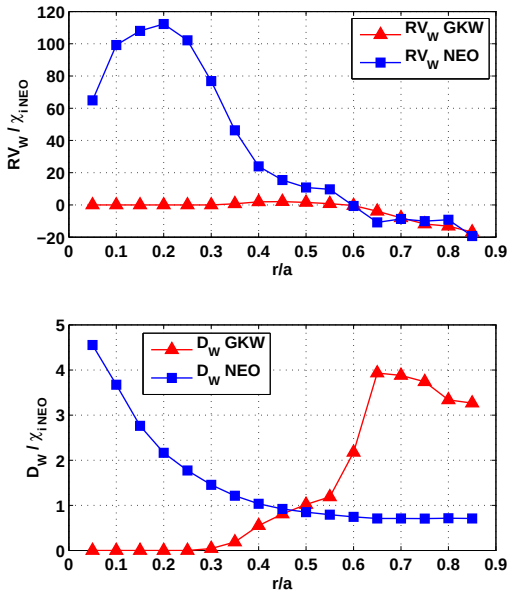

Fig. 1a. Neocl. and turb. contributions in Eq. 1 for case at 5.9s

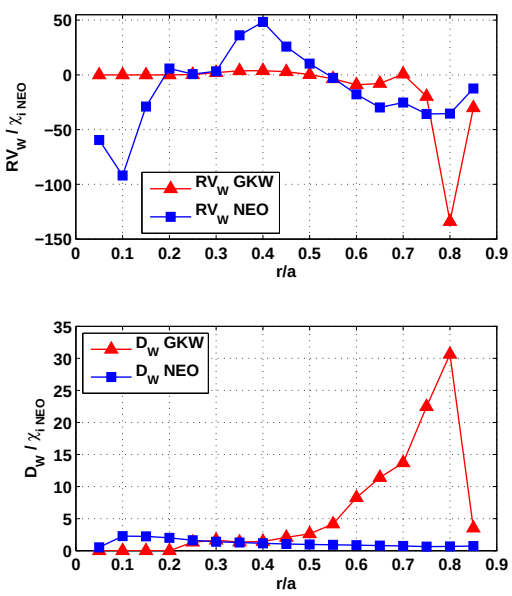

Fig. 1b. Neocl. and turb. contributions in Eq. 1 for case at 7.5s

of R/L_{nW} reads

$$\frac{R}{L_{nW}} = -\frac{\frac{\chi_{i\,an}}{\chi_{i\,\mathrm{NEO}}}\frac{RV_{W\,\mathrm{GKW}}}{\chi_{i\,\mathrm{GKW}}} + \frac{RV_{W\,\mathrm{NEO}}}{\chi_{i\,\mathrm{NEO}}}}{\frac{\chi_{i\,an}}{\chi_{i\,\mathrm{NEO}}}\frac{D_{W\,\mathrm{GKW}}}{\chi_{i\,\mathrm{GKW}}} + \frac{D_{W\,\mathrm{NEO}}}{\chi_{i\,\mathrm{NEO}}}}, \tag{1}$$

The normalization to the ion heat conductivity used in this expression is appropriate for these cases, where the ion heat flux is dominant and, consistently, ITG instabilities have been found to dominate the linear spectrum. The four terms of Eq. (1) are plotted in Fig. 1 for the two time slices (GKW results are plotted with the normalizations included in Eq. 1, that is $D_{W\,\mathrm{GKW}}/\chi_{i\,\mathrm{NEO}} = (D_{W\,\mathrm{GKW}}/\chi_{i\,\mathrm{GKW}})(\chi_{i\,an}/\chi_{i\,\mathrm{NEO}})$ and analogous expression for $RV_{W\,\mathrm{GKW}}/\chi_{i\,\mathrm{NEO}}$). Although the ratio $(\chi_{i\,an}/\chi_{i\,\mathrm{NEO}})(D_{W\,\mathrm{GKW}}/\chi_{i\,\mathrm{GKW}})$ appearing at the denominator of Eq. (1) becomes significantly larger than the corresponding neoclassical term $D_{W\,\mathrm{NEO}}/\chi_{i\,\mathrm{NEO}}$ at $r/a > 0.5$, the neoclassical pinch component $RV_{W\,\mathrm{NEO}}/\chi_{i\,\mathrm{NEO}}$ is never negligible in these plasmas. Actually, it provides the dominant contribution, particularly in the central region $r/a < 0.3$, and determines the predicted W behaviour. The strong neoclassical inward convection at 7.5 s is produced by the central peaking of the plasma density profile in this later phase [7]. The 2D density distribution of W over the poloidal cross-section can be built from the LFS profile of R/L_{nW} computed with Eq. (1), by integration over the radial direction taking into account the poloidal asymmetry produced by centrifugal effects [10,3,4]. The results are presented in Fig. 2, and clearly show the W localization at the LFS at 5.9s due to centrifugal trapping in the presence of a hollow LFS W density profile, and an extreme central peaking at 7.5 s, produced by neoclassical accumulation. The radial profiles of the transport coefficients obtained by the combination of NEO and GKW results are found to reproduce the main features of the W transport empirically obtained by an analysis with the JETTO/SANCO transport package [7]. The predicted 2D density distributions presented in Fig. 2 reproduce the main features observed on the poloidal cross–section of the SXR emission obtained by tomographic inversion of the SXR signals of the JET discharge under study.

2. W behaviour in JET-ILW hybrid plasmas

We investigate here how generic are the results obtained by the specific modelling of shot ♯82722 and if signatures of neoclassical transport accumulation are observed in general in these JET-ILW hybrid plasmas. A common feature of these hybrid scenarios is the development of a transient phase featuring a hollow density profile after the NBI switch-on and the consequent transition to H–mode [7]. Hollow main plasma density

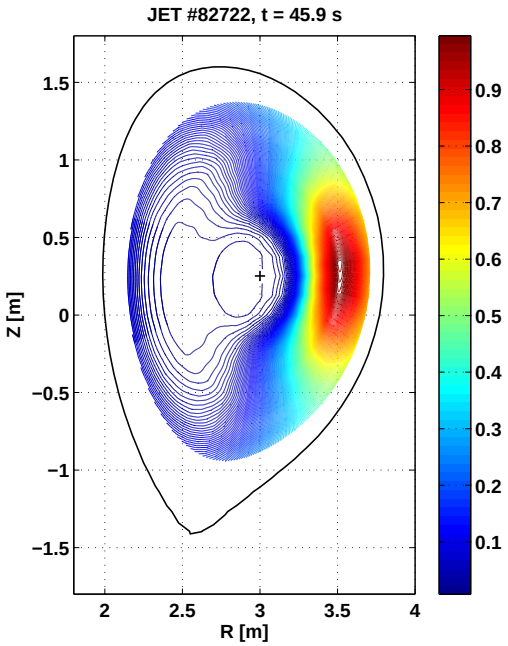

Fig. 2a. Predicted contour lines of W density (normalized to max = 1) at 5.9s

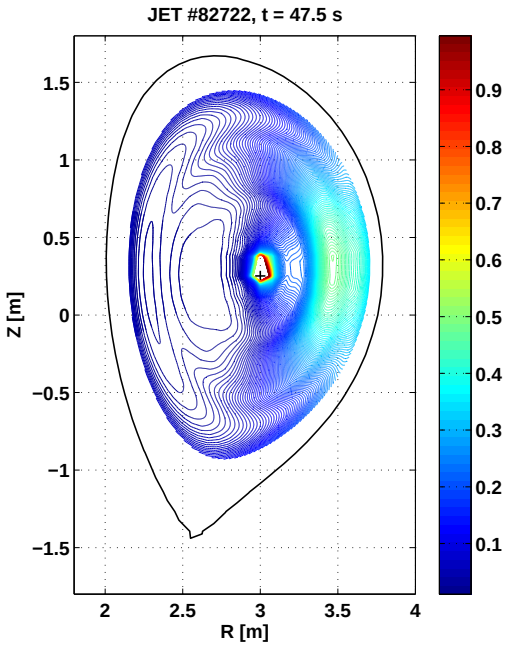

Fig. 2b. Predicted contour lines of W density (normalized to max = 1) at 7.5s

profiles are favorable to avoid neoclassical accumulation, but this condition is only transient, and eventually in these discharges the main plasma density peaks in the center. In almost the totality of cases, also W is observed to peak, following the behaviour of the electron density. This suggests an important role of neoclassical W transport in the accumulation process, consistently with the theory modelling results presented in the previous section. The comparison between conditions which lead to W accumulation with those in which W accumulation is not observed reveal that the critical radial window in which the peaking of the main plasma density profile is related to W accumulation is inside r/a = 0.3. The time evolution of the central peaking of the W density can be monitored with a proxy given by the ratio of the SXR signal of a central line of sight (LOS) to that of a peripheral LOS, appropriately normalized to the ratio of the chord lengths and to the ratio of the electron density at the magnetic surfaces to which the LOS are tangent (practically the magnetic axis for the central LOS t19, and $r/a = 0.4$ for the peripheral LOS t25). In Fig. 3, the time evolution of this proxy for the W peaking is plotted against a local parameter $R/L_{ni} - 0.5R/L_{Ti}$ at $r/a = 0.15$, which is proportional to a simple analytical estimate of the neoclassical pinch to diffusivity ratio of W [11] (R/L_{ne} and R/L_{Te} are used in place of R/L_{ni} and R/L_{Ti} respectively, since Ti measurements are not available on a regular basis for these plasma discharges). The large majority of the discharges follow more or less the same curve in this space of variables, which provides strong indication that neoclassical transport is the main mechanism responsible for the observed accumulation, consistently with the theory-based modelling results of discharge 82722 presented in the previous section. We note that some of these plasma discharges in hybrid scenario develop NTM (3/2, 4/3 or 5/4), and interesting correlations in time are observed in some cases between the appearance of the NTM and an increase in the peaking rate of W [12]. We speculate that there is an unfavorable interaction between the neoclassical transport and the development of an island, when the island appears in the presence of a hollow LFS density profile of W (like that predicted in Fig. 2a). In these conditions, the impact of the island is to move W rapidly inward, in a more central region where the neoclassical transport is more unfavorable and can more efficiently lead to accumulation. We provide some evidence in support of this speculation by plotting in Fig. 4 the change in W peaking rate (estimated simply as $d\log(t_{19}/t_{25})/dt$) as a function of the proxy of the W peaking already used in Fig. 3, evaluated at the appearance of

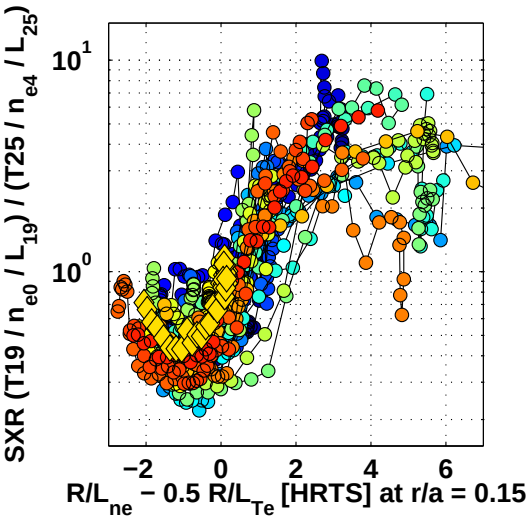

Fig. 3. Proxy of W LFS peaking vs proxy of neoclassical pinch to diffusion ratio

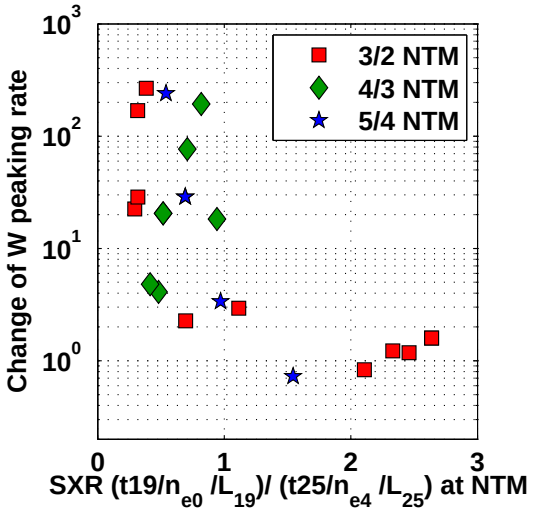

Fig. 4. Change of peaking rate after the appearance of a NTM vs a proxy of the W LFS density peaking

the NTM. In the cases where the NTM appears in the presence of a centrally peaked W LFS density, small changes in the W peaking rate are observed. In contrast, when the W LFS density is hollow, the change in peaking rate can be extremely large. Finally, in some discharges, $n = 1$ activity can prevent the build up of strong central gradients of the main plasma density, with the beneficial effect of reducing the neoclassical pinch (e.g. shot ♯83527) (see also [7,13]).

3. Conclusions

Neoclassical DK (NEO) and linear GK (GKW) calculations of W transport during an early and a late time-slice of the high power phase of a JET-ILW hybrid scenario discharge reproduce the main features of the W behaviour observed in the experiment. In the early phase a centrally hollow LFS W density profile is predicted, with consequent off-axis LFS localization of W due to centrifugal effects. In contrast, in the later phase, an extreme central peaking of W is produced by neoclassical accumulation due to the central peaking of the plasma density. These results indicate that W accumulation in the core is mainly determined by the dominant role of neoclassical transport in the central region of the plasma ($r/a < 0.3$) (see also [7]). This conclusion appears to be confirmed by the analysis of a dataset of plasma discharges in hybrid scenario, where the time evolution of a proxy of the W peaking is found to be highly correlated with a simple analytical estimate of the neoclassical pinch to diffusion ratio in the center ($r/a \simeq 0.15$). In some cases MHD modes significantly impact this time evolution. It is suggested that when NTMs appear where the LFS W density profile is hollow, they can produce a fast displacement of a significant amount of the off-axis localized W toward a more internal region where neoclassical transport is more unfavorable, with consequent faster accumulation.

Acknowledgments. This work was supported by EURATOM and carried out within the framework of the European Fusion Development Agreement. The views and opinions expressed herein do not necessarily reflect those of the European Commission.

[1] Pütterich T. *et al* 2013 this conf., I2.106. [2] Camenen Y. *et al* 2009 *Phys. Plasmas* **16** 012503. [3] Casson F. J. *et al* 2010 *Phys. Plasmas* **17** 102305. [4] Angioni C. *et al* 2011 *Nucl. Fusion* **51** 023006. [5] Angioni C. *et al* 2012 *Phys. Plasmas* **19** 122311. [6] Casson F. J *et al* 2013 *Nucl. Fusion* **53** 063026. [7] Mantica P. *et al* 2013 this conf., P4.141. [8] Belli E. and Candy J. 2008 *Plasma Phys. Control. Fusion* **50** 095010, 2012 *Plasma Phys. Control. Fusion* **54** 015015. [9] Peeters A.G. *et al* 2009 *Comput. Phys. C.* **180** 2650. [10] Hinton F.L. and Wong S.K. 1985 *Phys. Fluids* **28** 3082. [11] Hirshman S.P. and Sigmar D.J. 1981 *Nucl. Fusion* **21** 1079. [12] Hender T.C. 2013 priv. comm. and Baruzzo M. *et al* 2013 this conf., P5.161. [13] Baranov Y. *et al* 2013 this conf., P5.142.